Korea-Australia Rheology Journal
Vol. 14, No. 4, December 2002 pp. 175-188

Fiber orientation in the processing of polymer composites

Du Hwan Chung and Tai Hun Kwon*
Department of Mechanical and Industrial Engineering, Pohang University of Science and Technology, San 31 Hyojadong, Nam-ku, Pohang, Kyungbuk 790-784, Korea
(Received June 6, 2002)

Abstract

We review the modeling and simulation of fiber orientation during injection molding processes of short fiber reinforced thermoplastics. Generally, a group of fibers are described in terms of probability distribution function or orientation tensor. Various closure approximation models to express higher order tensor in terms of lower order tensors are reviewed. Rheology of fiber suspensions, multiple fiber-fiber interaction and numerical technique for the prediction of fiber orientation are also considered for concentrated situations.

1. Introduction

Short-fiber reinforced composites are widely used for their high strength to weight ratios and remarkably enhanced physical properties compared with pure polymer products. Compression molding, extrusion, and injection molding are some of the processes often used. The fibers are suspended in the polymer matrix, and orient themselves in response to the interactions among kinematics of the flow, other neighboring fibers and mold cavity. Fiber reinforced composite typically shows anisotropic mechanical, thermal and rheological properties. Prediction of thermo-mechanical properties with given fiber orientation has been well developed to some extent (Halpin and Kardo, 1976). Therefore, prediction of fiber orientation during the transient mold filling is important for the prediction of such anisotropic properties of final plastic part. There have been considerable interests in the evolution of the distribution of the orientation of fibers, and the bulk stress for given flow and instantaneous microstructure, especially for non-dilute suspensions.

For the effective design of short-fiber reinforced polymer-based composites, CAE (Computer Aided Engineering) can play a important role. Because of highly nonlinear and complex flow characteristics of polymer and particle-contained suspensions, only numerical solutions including appropriate models are manageable. This economic technique offers a detail understanding of the process and aids in identifying the cause of the problems rather than time- consuming trial-and-error experiments. However, most commercial packages use rather simplified models and numerical algorithms, which are not accurate, to calculate fiber orientation distribution. Therefore, the modeling and numerical prediction of fiber suspension is the field where there are much current research activities.

2. Fiber orientation

Motion of a single rigid ellipsoidal particle immersed in a viscous Newtonian liquid was considered by (Jeffery, 1922). Evolution equation for a single rigid ellipsoidal particle was developed, and it is the starting point of almost all the fiber orientation constitutive modeling. Fiber suspensions are characterized in terms of the number of fibers per unit volume n, fiber length L and diameter D as dilute ($nL^3<<1$), semi-dilute ($nL^3>>1$, $nL^2D<<1$) and concentrated ($nL^3>>1$, $nL^2D>>1$) regime. nL^3 means the number of interacting fibers in a volume swept by a single fiber and nL^2D means an excluded volume of interacting fibers due to a line approximation of a fiber.

Nowadays, many researchers have developed many numerical simulation programs with different methods for the description of fiber orientation including multiple fiber-fiber interaction. However, some of them using direct calculation of fiber motion (Yamamoto and Matsuoka, 1993), (Yamane *et al*., 1994), (Mackaplow and Shaqfeh, 1996), (Sundararajakumar and Koch, 1997), (Fan *et al*., 1998) require incredible computation time which is the reason why such a numerical simulation method cannot be accommodated. Calculation of fiber orientation state using the probability distribution function (DFC, in short) is one of them. Instead, a tensor representation of orientation state (Advani and Tucker, 1987), which is a pre-averaging concept of DFC, is widely used for its efficiency, compactness and above all, manageable computation time. However, it is necessary to introduce a closure approximation to express the higher order tensor in terms of lower order tensors for a closed set of equation since the evolution equa-

*Corresponding author: thkwon@postech.ac.kr

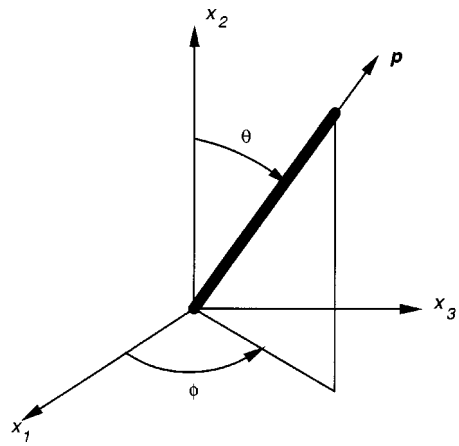

Fig. 1. Orientation of a single fiber.

tion for orientation tensor involves the next higher even order tensor.

2.1. Probability distribution function

The orientation state of a group of fibers can be described by a probability distribution function $\Psi(\boldsymbol{p})$ (Advani and Tucker, 1987), which provides a general description of the orientation state. With the assumptions of rigid cylindrical fibers, mono-disperse distribution in fiber length and diameter, and spatially uniform concentration, the orientation of a single fiber can be described by a unit vector $\boldsymbol{p}$ as shown in Fig. 1. Also, components of $\boldsymbol{p}$ can be represented by spherical coordinates of angles θ and ϕ.

The probability of finding a fiber between angles θ_1 and $\theta_1 + d\theta$, and ϕ_1 and $\phi_1 + d\phi$, is given by

$$P(\theta_1 \le \theta \le \theta_1 + d\theta, \phi_1 \le \phi \le \phi_1 + d\phi) = \Psi(\theta_1, \phi_1)\sin\theta_1 d\theta d\phi \quad (1)$$

The integration of this function over orientation space must equal to unity (the normalization condition):

$$\int_{\phi=0}^{2\pi}\int_{\theta=0}^{\pi} \Psi(\theta,\phi)\sin\theta d\theta d\phi = \oint \Psi(\boldsymbol{p})d\boldsymbol{p} = 1 \quad (2)$$

A fiber oriented at any angle (θ, ϕ) is indistinguishable from a fiber oriented at any angle $(\pi - \theta, \phi + \pi)$, so Ψ must be even, in the sense that

$$\Psi(\theta, \phi) = \Psi(\pi - \theta, \phi + \pi) \text{ or } \Psi(\boldsymbol{p}) = \Psi(-\boldsymbol{p}) \quad (3)$$

With the assumption that fibers move with the bulk motion of the fluid, Ψ may be regarded as a convected quantity. The continuity equation (conservation equation of probability) is then

$$\frac{D\Psi}{Dt} = -\frac{\partial}{\partial\theta}(\dot{\theta}\Psi) - \frac{1}{\sin\theta}\frac{\partial}{\partial\phi}(\dot{\phi}\Psi) \text{ or } \frac{D\Psi}{Dt} = -\frac{\partial}{\partial\boldsymbol{p}}\cdot(\Psi\dot{\boldsymbol{p}}) \quad (4)$$

If an appropriate expression for the fiber angular velocity, $\dot{\boldsymbol{p}}$, is given, Eq. (4) becomes the evolution equation for the probability Ψ. Solving the orientation states via the probability distribution function $\Psi(\boldsymbol{p})$ is called the "Distribution Function Calculation", DFC in short. Although the calculation of DFC can be done using any numerical techniques, it requires tremendous computational efforts. Thus, one needs a more compact and efficient description of orientation state to be used in practical or commercial processing situations.

2.2. Orientation tensors

Orientation tensors (Advani and Tucker, 1987) are widely used to provide a more compact representation of the fiber orientation state in order to improve computational efficiency. Orientation tensors are defined as the dyadic products of $\boldsymbol{p}$ averaged over orientation space, with Ψ as the weighting function. Because the distribution function is even, the odd-order tensors are all zero.

The second and fourth order orientation tensors are defined as follows:

$$a_{ij} = \int p_i p_j \Psi(\boldsymbol{p})d\boldsymbol{p}, \quad a_{ijkl} = \int p_i p_j p_k p_l \Psi(\boldsymbol{p})d\boldsymbol{p} \quad (5)$$

Completely symmetric properties are as follows;

$$a_{ij} = a_{ji}$$

$$a_{ijkl} = a_{jikl} = a_{kijl} = a_{lijk}, \quad \text{etc.} \quad (6)$$

The normalization can be expressed by following Eq.(7) ;

$$a_{ii} = 1, \quad a_{ijkk} = a_{ij} \quad (7)$$

Due to symmetry (Eq. 6) and normalization conditions (Eq. 7), only five independent components of a_{ij} and fourteen independent components of a_{ijkl} exist.

Orientation tensor components have a physical interpretation. Fig. 2(a) shows isotropic orientation state, with equal orientation distribution in all directions. If all the fibers lie in the 1-2 plane in isotropic state [Fig. 2(b)], it corresponds to planar random (2D isotropic) orientation state. Perfectly aligned orientation in x_1 direction is shown in Fig. 2(c).

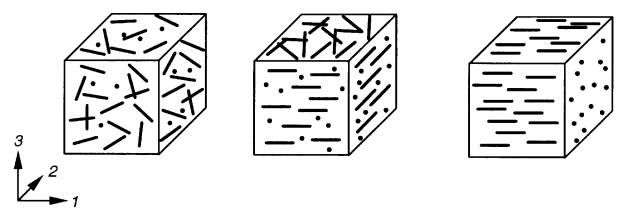

$$a_{ij} = \begin{bmatrix} 1/3 & 0 & 0 \\ 0 & 1/3 & 0 \\ 0 & 0 & 1/3 \end{bmatrix} \quad a_{ij} = \begin{bmatrix} 1/2 & 0 & 0 \\ 0 & 1/2 & 0 \\ 0 & 0 & 0 \end{bmatrix} \quad a_{ij} = \begin{bmatrix} 1 & 0 & 0 \\ 0 & 0 & 0 \\ 0 & 0 & 0 \end{bmatrix}$$

(a) 3-D random (b) planar random (c) aligned

Fig. 2. Example of different orientation states and corresponding orientation tensors.

2.2.1. Isotropic diffusivity

The fiber angular velocity $\dot{p}_i$ with isotropic diffusivity constant D_r (Folgar and Tucker, 1984) is as follows:

$$\dot{p}_i = -\frac{1}{2}\omega_{ij}p_j + \frac{1}{2}\lambda(\dot{\gamma}_{ij}p_j - \dot{\gamma}_{kl}p_k p_l p_i) - \frac{D_r}{\Psi}\frac{\partial \Psi}{\partial p_i} \tag{8}$$

The evolution equation for the second order orientation tensor a_{ij} can be expressed as (Advani and Tucker, 1987)

$$\frac{Da_{ij}}{Dt} = -\frac{1}{2}(\omega_{ik}a_{kj} - a_{ik}\omega_{kj}) + \frac{1}{2}\lambda(\dot{\gamma}_{ik}a_{kj} + a_{ik}\dot{\gamma}_{kj} - 2\dot{\gamma}_{kl}a_{ijkl}) + 2D_r(\delta_{ij} - 3a_{ij})$$

$$\lambda = \left(\frac{(L/D)^2 - 1}{(L/D)^2 + 1}\right) \tag{9}$$

where $\omega_{ij} = u_{j,i} - u_{i,j}$ is the rotation rate tensor, $\dot{\gamma}_{ij} = u_{j,i} + u_{i,j}$ is the rate of deformation tensor, and δ_{ij} is the identity tensor. λ is a parameter related to the aspect ratio of the fiber L/D. The third term on the right hand side of Eq. (9) accounts for the fiber-fiber interaction. In concentrated suspensions, the rotary diffusivity term D_r is used to model the fiber-fiber interaction. Folgar and Tucker (1984) suggested $D_r = C_I\dot{\gamma}$. However, established model for the prediction of an interaction coefficient C_I does not exist, yet. Therefore, C_I is used for an empirical value that must be determined by comparing predictions with experiments. $\dot{\gamma}$ is the generalized shear rate, defined as

$$\dot{\gamma} = \sqrt{\frac{1}{2}\dot{\gamma}_{ij}\dot{\gamma}_{ji}} \tag{10}$$

2.2.2. Anisotropic diffusivity

One can introduce anisotropic diffusivity in the randomizing effect on the probability distribution function. The fiber angular velocity $\dot{p}_i$ with anisotropic tensor D_{ij} is as follows:

$$\dot{p}_i = -\frac{1}{2}\omega_{ij}p_j + \frac{1}{2}\lambda(\dot{\gamma}_{ij}p_j - \dot{\gamma}_{kl}p_k p_l p_i) - \frac{D_{ij}}{\Psi}\frac{\partial \Psi}{\partial p_j} \tag{11}$$

The evolution equation for the second order orientation tensor a_{ij} can be expressed as

$$\frac{Da_{ij}}{Dt} = -\frac{1}{2}(\omega_{ik}a_{kj} - a_{ik}\omega_{kj}) + \frac{1}{2}\lambda(\dot{\gamma}_{ik}a_{kj} + a_{ik}\dot{\gamma}_{kj} - 2\dot{\gamma}_{kl}a_{ijkl}) + 2(D_{ij} - D_{kk}a_{ij}) - 3(D_{ik}a_{kj} + D_{jk}a_{ki}) + 6D_{lm}a_{lmij} \tag{12}$$

To implement Eq. (12), another closure model for fourth-order orientation tensor must be developed. Also, how to determine D_{ij} remains with question. In this regard, no complete study has been available along this direction.

3. Closure approximation

Various closure approximations have been proposed. Among them, a Hybrid closure approximation (HYB) (Advani and Tucker, 1990) has readily been used for its stable behaviors in spite of its over-prediction of orientation components compared with DFC. Recently, (Cintra and Tucker, 1995) developed Orthotropic fitted closure approximation (ORF, ORL) by assuming that the principal directions of 4th order orientation tensor are functions of the eigenvalues of 2nd order orientation tensor. Unknown parameters were determined by fitting selected flow data obtained from DFC. ORF (or ORL) shows better behaviors than previous closure approximations but unfortunately suffers from non-physical oscillations at low value of fiber-fiber interaction coefficient. Chung and Kwon have proposed (ORW, 1999; ORW3, 2001), which overcome such problems of non-physical oscillations. However, such Orthotropic type closure approximations (ORF, ORL, ORW and ORW3) requires additional computation time for the transformation between the global coordinate system and the principal coordinate system. In this respect, (Chung and Kwon, 2002a) have proposed IBOF (Invariant Based Optimal Fitting) closure approximation, which significantly reduces the computation time

3.1. Hybrid closure approximation (HYB)

One of the popular models used in the numerical simulation of real manufacturing processes, such as injection molding, compression molding, is the hybrid closure approximation (HYB) (Advani and Tucker, 1990), since it shows stable behavior of fiber orientation state with reasonable computational efficiency. HYB is a combination of linear (LIN) and quadratic (QUA) closure approximation, summarized by the following equations:

3.1.1. Linear closure approximation (LIN)

$$\hat{a}_{ijkl} = -\frac{1}{35}(\delta_{ij}\delta_{kl} + \delta_{ik}\delta_{jl} + \delta_{il}\delta_{jk}) + \frac{1}{7}(a_{ij}\delta_{kl} + a_{ik}\delta_{jl} + a_{il}\delta_{jk} + a_{kl}\delta_{ij} + a_{jl}\delta_{ik} + a_{jk}\delta_{il}) \tag{13}$$

3.1.2. Quadratic closure approximation (QUA)

$$\tilde{a}_{ijkl} = a_{ij}a_{kl} \tag{14}$$

3.1.3. Hybrid closure approximation (HYB)

$$\bar{a}_{ijkl} = (1-f)\hat{a}_{ijkl} + f\tilde{a}_{ijkl} \tag{15}$$

$$f = 1 - 27\det[a_{ij}]$$

where f represents the scalar measure of orientation.

It is well known that HYB tends to consistently over-predict the flow-induced fiber orientation states compared with DFC for most flow cases (Advani and Tucker, 1990), (Bay, 1992a; 1992b), (Chung and Kwon, 1995; 1996), (Chung and Kwon, 2000).

3.2. Eigenvalue-based optimal fitting (EBOF) model

3.2.1. Orthotropic fitted closure approximation (ORF, ORL)

The orthotropic closure approximation was defined to

satisfy the orthotropic assumption that non-zero principal fourth-order orientation tensor components in the eigenspace system, with full symmetry conditions, are a^p_{1111}, a^p_{2222} $a^p_{3333}, a^p_{1122}, a^p_{2233}, a^p_{1133}$ (Cintra and Tucker, 1995). The superscript p refers to the eigenspace system in the present paper. There are only three independent components among the six non-zero components, due to the full symmetry and normalization conditions that apply.

The six non-zero components can be denoted in contracted notation by $\overline{A}_{ii}$:

$$\overline{A}_{11} = a^p_{1111},\ \overline{A}_{22} = a^p_{2222},\ \overline{A}_{33} = a^p_{3333},\ \overline{A}_{44} = a^p_{1122},\ \overline{A}_{55} = a^p_{2233}$$
$$\overline{A}_{66} = a^p_{3311} \tag{16}$$

These equations are assumed to depend on the eigenvalues of a_{ij} (Cintra and Tucker, 1995). In particular, ORF and ORL take the following polynomial functional forms:

$$\overline{A}^{closure}_{mm} = C^1_m + C^2_m a_1 + C^3_m [a_1]^2 + C^4_m a_2 + C^5_m [a_2]^2 + C^6_m a_1 a_2\,,$$
$$m = 1,\ldots,3 \text{ (no sum on m)} \tag{17}$$

where a_1 and a_2 are the two largest eigenvalues of a_{ij} (i.e., $a_1 \geq a_2 \geq a_3$). Once $\overline{A}_{11}$, $\overline{A}_{22}$ and $\overline{A}_{33}$ are determined, $\overline{A}_{44}$, $\overline{A}_{55}$ and $\overline{A}_{66}$ can be calculated by applying the normalization conditions. Eighteen C^k_m (k = 1,.....,6) parameters were determined using a least square optimal fit with the presumed exact fiber orientation solutions from the DFC for several flows.

The ORF and ORL are quite successful in predicting most simple homogeneous and non-homogeneous flows, and are regarded as a significant improvement in the closure approximation literature. However, for low C_I values, the ORF and ORL suffer from non-physical oscillations when used for simple shear and radial diverging flows.

3.2.2. Modified hybrid closure approximation

Han and Im (1999) improved previous HYB by enforcing extreme orientation of random-in-space, random-in-plane, uniaxial states into the model. Orientation Distribution Function form was assumed by intuition and was fitted using DFC. Principal fourth-order orientation tensor components were expressed in terms of eigenvalues of second-order orientation tensor. The accuracy was not that satisfactory as compared with ORF or ORL and the necessity of considerable computation time of coordinate transformation is indispensable.

3.2.3. ORW and ORW3

The ORW and ORW3 (Chung, 1999 and Kwon, 2001) were proposed as an improvement to the ORF and ORL to overcome non-physical oscillations. This was achieved by introducing fitted flow data that covers the entire range of fiber orientation states, in particular the combined shear/planar-elongation flow resembling radial diverging flow. Representative values of $\lambda = 1$, $C_I = 0.0001$ were chosen for the fiber-orientation modeling of injection-molded composites. The functional form for the ORW is the same as those used for ORF or ORL, whereas the ORW3 assumes a third order polynomial expansion of a_1, a_2 in Eq. (17). The ORW3 performs better than ORW, especially for non-homogeneous radial diverging flows with low C_I values.

3.2.4. ORE

Verweyst (1998) and Wetzel (1999) recently introduced another version of orthotropic fitted closure approximations, ORE, that differs from ORF (or ORL) in that analytical solutions corresponding to $C_I = 0$ and $\lambda = 1$ were adopted for the fitting, similar to the procedure used for the NAT approximation. Also, the fourth order complete polynomial of a_1, a_2 is used in Eq. (17). The performance of the ORE is almost as good as ORW3.

3.3. Invariant-based system

3.3.1. Natural (NAT) closure approximation

The NAT is an invariant-based system, since a general expression for a_{ijkl}, in terms of a_{ij} and δ_{ij}, and polynomial expansions in terms of the principal invariants of a_{ij}, are used for the unknown coefficients in the general expression. The term "natural" originated from the fact that the NAT uses natural closure values: analytical solutions that exist only for $C_I = 0.0$ with $\lambda = 1$ in a least square fitting procedure (Verleye and Dupret, 1994). It exhibits good transient behavior, but over-predicts steady state orientations compared with DFC, slightly. Singularities do exist, which is a significant drawback; the singularities must be treated with special care when applying the NAT to general flows (Dupret and Verleye, 1999).

3.3.2. Invariant Based Optimal Fitting closure approximation (IBOF)

IBOF (Chung and Kwon, 2002a) also starts with the most general expression of a full symmetric 4th order tensor a_{ijkl} in terms of a_{ij} and δ_{ij} as follows :

$$a_{ijkl} = \beta_1 S(\delta_{ij}\delta_{kl}) + \beta_2 S(\delta_{ij}a_{kl}) + \beta_3 S(a_{ij}a_{kl}) + \beta_4 S(\delta_{ij}a_{km}a_{ml}) + \beta_5 S(a_{ij}a_{km}a_{ml}) + \beta_6 S(a_{im}a_{mj}a_{kn}a_{nl}) \tag{18}$$

where the operator S indicate the symmetric part of its argument, for instance,

$$S(T_{ijkl}) = \frac{1}{24}(T_{ijkl} + T_{jikl} + T_{ijlk} + T_{jilk} + T_{klij} + T_{lkij} + T_{klji} + T_{lkji} + T_{ikjl} + T_{kijl} + T_{iklj} + T_{kilj} + T_{jlik} + T_{ljik} + T_{jlki} + T_{ljki} + T_{iljk} + T_{lijk} + T_{ilkj} + T_{likj} + T_{jkil} + T_{kjil} + T_{jkli} + T_{kjli}) \tag{19}$$

IBOF assumes that the coefficients $\beta_1 \sim \beta_6$ are polynomial expansions of the second and third invariants (II, III) of a_{ij}. It can be easily shown that, among the six β_i's in Eq.(18), there are only three independent values with the rest being determined in terms of the three independent ones with the help of the normalization conditions and full symmetry between indices together with Cayley-Hamilton Theorem.

IBOF predicts fiber orientation behavior as accurately as EBOF for all of the flow fields tested, over a wide range of C_I. EBOF models (ORF, ORL, ORW, ORW3) requires additional computation time for the transformation between the global coordinate and principal coordinate and most of times are spent for this procedure. IBOF does not require such computation and total CPU time is about 30~40% the computation time EBOF models require for the same situations.

3.4. Performance of closure approximations

For a benchmark test problem of non-homogeneous isothermal Newtonian radial diverging flow field, the velocity field is represented by

$$u_r = \frac{3Q}{8\pi rb}\left(1-\frac{z^2}{b^2}\right), \qquad u_\theta = u_z = 0 \tag{20}$$

where Q is volume flow rate, b is the half-gap thickness, r is the radial-direction and z is the thickness-direction. Using a local Cartesian coordinate system in which the (1, 2, 3) axes correspond to (r, θ, z), the velocity gradients are

$$\frac{\partial u_i}{\partial x_j} = \frac{3Q}{8\pi rb}\begin{bmatrix} -\frac{1}{r}\left(1-\frac{z^2}{b^2}\right) & 0 & -\frac{2}{b}\left(\frac{z}{b}\right) \\ 0 & \frac{1}{r}\left(1-\frac{z^2}{b^2}\right) & 0 \\ 0 & 0 & 0 \end{bmatrix} \tag{21}$$

The flow is in the 1-direction, with stretching in the 2-direction and shearing across the 3-direction. This makes the non-homogeneous flow an ideal benchmark test case for the proposed closure approximation.

Prediction by DFC is supposed to provide exact solutions that can be compared with the predictions of any closure approximation to evaluate their performance.

Fig. 3 shows the a_{11} component (the flow directional orientation component) as a function of the normalized radial location (r/b) at several gap-wise thickness positions (z/b) for DFC, HYB, ORF, ORL in the case of C_I = 0.001. HYB (Fig. 3b) obviously makes an over-prediction in comparison with DFC (Fig. 3a), as is generally known. Both ORF

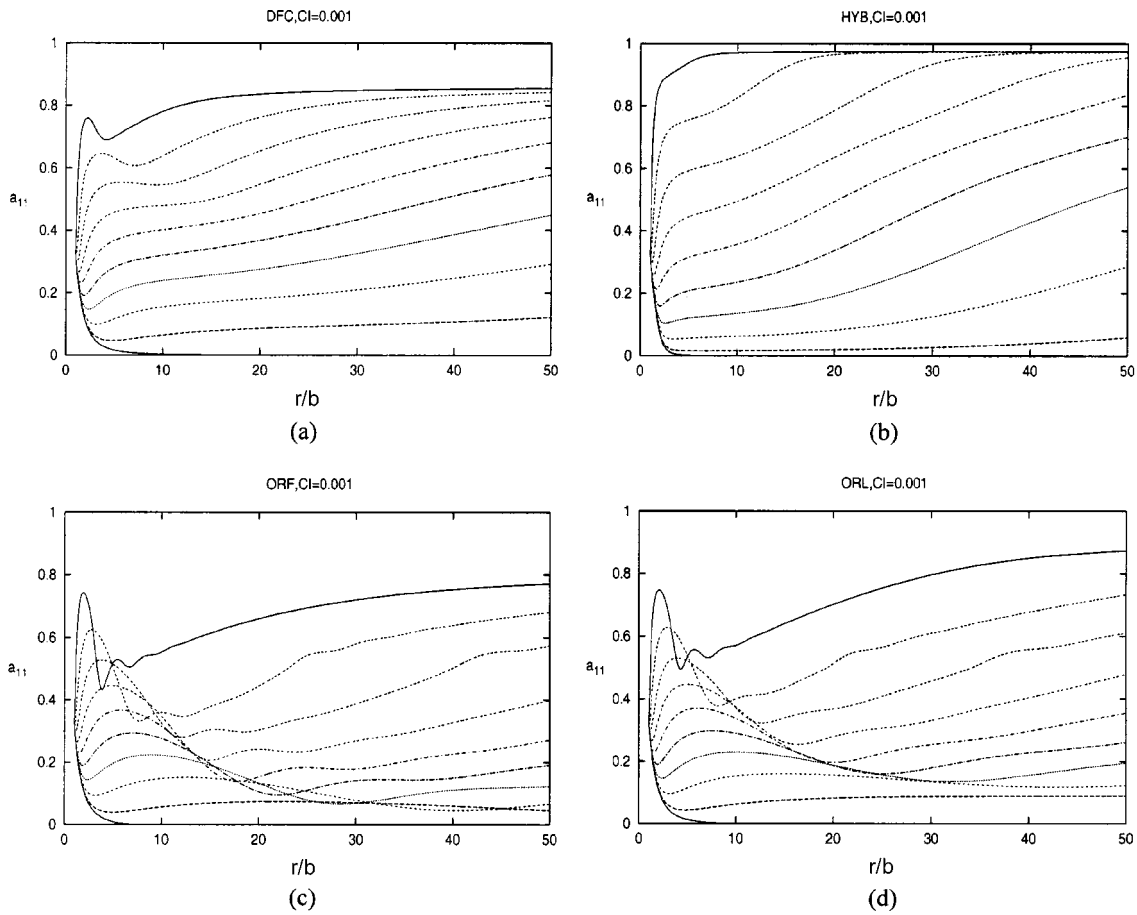

Fig. 3. a_{11} component in isothermal Newtonian radial diverging flow as a function of radial location (r/b) at several thickness positions (z/b) (z/b = 0.9, 0.8, 0.7, 0.6, 0.5, 0.4, 0.3, 0.2, 0.1, 0.0 from the top to botton curves) for various closure approximations with C_I=0.001: (a) DFC, (b) HYB, (c) ORF, (d) ORL.

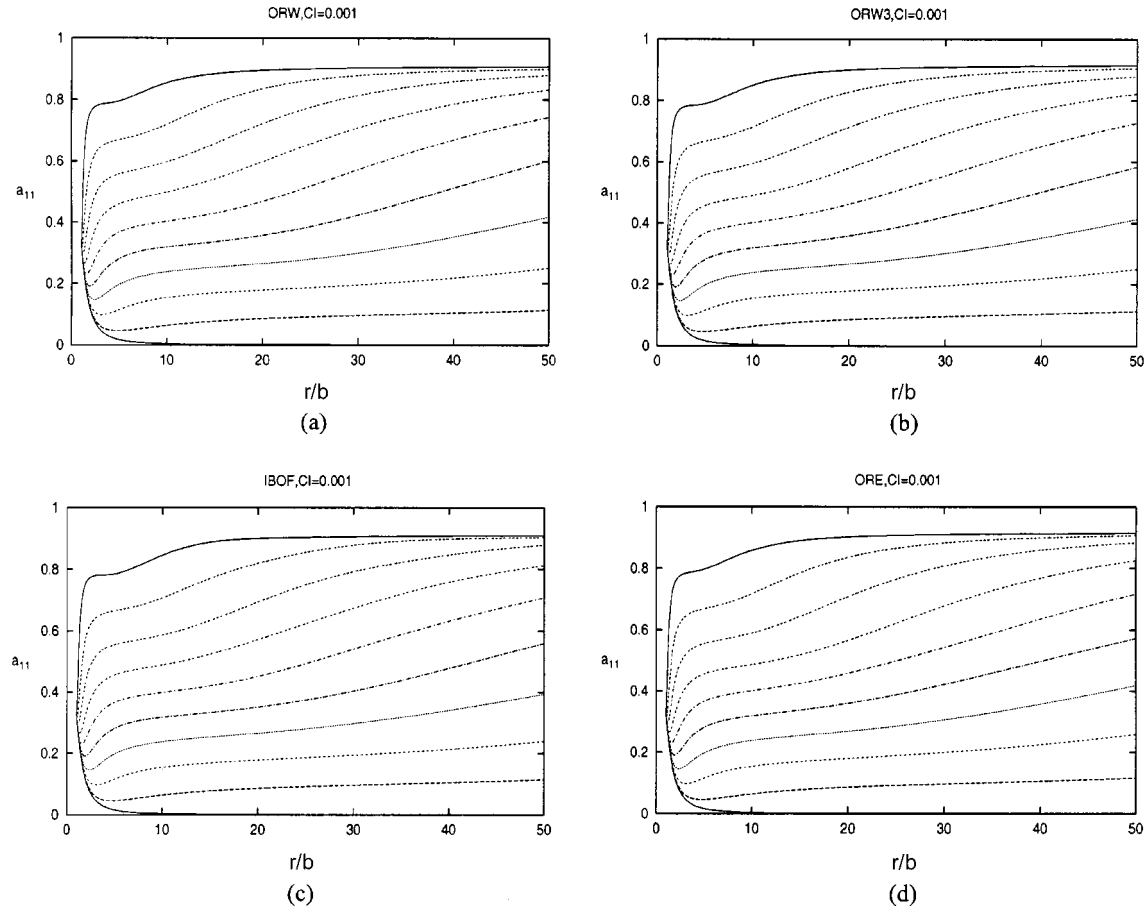

Fig. 4. a_{11} component in isothermal Newtonian radial diverging flow as a function of radial location (r/b) at several thickness positions (z/b) for various closure approximations with C_I=0.001: (a) ORW, (b) ORW3, (c) IBOF, (d) ORE. The meaning of curves is the same as that in Fig. 3.

and ORL clearly indicate non-physical oscillations in contrast to DFC for $C_I \leq 0.001$. It is certainly disappointing and thus is regarded as a critical defect. However, as shown in Fig. 4, ORW, ORW3, IBOF and ORE do not show any non-physical oscillations and are certainly in much better agreements with DFC than ORF or ORL for $C_I = 0.001$. Also, they slightly over-predict the flow directional orientation components compared with DFC at the shell (z/b = 0.6~0.9) layer, but match the DFC results in the core (z/b = 0.0~0.3) and transition (z/b = 0.3~0.6) layers fairly well.

4. Rheology of fiber suspensions

A general rheological constitutive equation for axisymmetric particles can be represented as follows:

$$\tau_{ij} = \eta\dot{\gamma}_{ij} + \eta\phi\{A\dot{\gamma}_{kl}a_{ijkl} + B(\dot{\gamma}_{ik}a_{kj} + a_{ik}\dot{\gamma}_{kj}) + C\dot{\gamma}_{ij} + 2Fa_{ij}D_r\} \quad (22)$$

where η is the solvent viscosity, ϕ is the particle volume fraction, A, B, C and F are geometric shape factor and D_r is the rotary diffusivity due to Brownian motion. For a slender particle, particle thickness can be ignored, producing B and C equal to zero. If the particle is large enough so that Brownian motion can be ignored, last term containing D_r can be omitted. Therefore, typical constitutive equation for fiber suspensions can be expressed as follows:

$$\tau_{ij} = \eta\dot{\gamma}_{ij} + \eta N u_{k,l}a_{ijkl} \quad (23)$$

where N represents anisotropic contribution of the fibers. Physically, it represents the amount by which the suspension resists elongation parallel to the fiber axial direction.

Most theoretical works have been done for dilute and semi-dilute suspensions, which deal with particle concentrations much below those required for technological applications. Typical dilute and semi-dilute bulk stress shows specific (or shear) viscosity to be linearly proportional to volume fraction. For semi-dilute suspensions, mechanism of hydrodynamic interaction and screening is well understood. Typically nL^2D is between 1 and 5 in the processing of fiber-reinforced composites by injection molding. Thus, consideration of concentrated regime, where direct

mechanical contacts between fibers are dominant, is of great practical importance. However, it has not been given much attention on this field. Therefore, more researches are necessary.

4.1. Dilute suspension

Batchelor (1971) derived following model considering the effect of fibers in dilute, semi-dilute suspension.

$$N = \frac{\pi n L^3}{6\ln(2L/D)} f(\varepsilon)$$

$$f(\varepsilon) = \frac{1+0.64\varepsilon}{1-1.5\varepsilon} + 1.659\varepsilon^2, \quad \varepsilon = [\ln(2L/D)]^{-1}. \tag{24}$$

Dilute suspensions of ellipsoidal fibers of large aspect ratio was considered as follows (Hinch and Leal, 1972).

$$N = \frac{\phi(L/D)^2}{[\ln(2L/D) - 1.5]} \tag{25}$$

4.2. Dilute suspension considering two body interactions

These are $O[nL^3]$ corrections to dilute suspensions and only aligned and isotropic orientation states were considered (Mackaplow and Shaqfeh, 1996; Shaqfeh and Fredrickson, 1990). Valid region is upto $nL^3 \sim O[\ln^2(2L/D)]$.

i) For aligned suspension

$$N = N^{dilute} + 8.583\times10^{-3}\frac{\pi(nL^3)^2}{\ln^3(2L/D)} \tag{26}$$

ii) For isotropic suspension

$$N = N^{dilute} + 9.25\times10^{-3}\frac{\pi(nL^3)^2}{\ln^3(2L/D)} \tag{27}$$

4.3. Semi-dilute suspension

Using Batchelors cell model (Batchelor, 1971), (Dinh and Armstrong, 1984) developed a rheological equation of state for semi-concentrated fiber suspensions where the average spacing h between neighboring fibers is greater than its diameter D, but less than its length L.

$$N = \frac{\pi n L^3}{6\ln(2h/D)} \tag{28}$$

$$h = \begin{cases} (nL^2)^{-1} \text{ for random orientation} \\ (nL)^{-1/2} \text{ for aligned orientation} \end{cases}$$

In the simulation, it is assumed that the average distance from a given fiber to its nearest neighbors h is linear in terms of the scalar measure of orientation f, which varies from zero to unity according to the orientation state of fibers. When the number of fibers per unit volume n is greater than $1/(DL^2)$, the average distance between fibers is assumed to be the same as for the aligned orientation state independent of the orientation state. Therefore, in this study, h is described as

$$h = (1-f)h_{random} + fh_{aligned} \text{ for } \frac{\pi}{4}\left(\frac{D}{L}\right)^2 < \phi < \frac{\pi}{4}\left(\frac{D}{L}\right)$$

$$h = h_{aligned} \text{ for } \frac{\pi}{4}\left(\frac{D}{L}\right) \le \phi < \frac{\pi}{4} \tag{29}$$

$$f = 1 - 27\det[a_{ij}]$$

where ϕ stands for the fiber volume fraction.

Dinh-Armstrong model predicts increased viscosity compared with theoretical value for randomly oriented suspension. In spite of this defect, it is widely used because of its simplicity.

Recently, Shaqfeh and Fredrickson (1990) proposed following model using diagrammatic representation of hydrodynamic interactions.

$$N = \frac{\pi n L^3}{3}\left\{\frac{1}{\ln(1/\phi) + \ln\ln(1/\phi) + C''}\right\} \tag{30}$$

where $C'' = -0.66$ for random orientation and $C'' = 0.16$ for aligned orientation. Screening mechanism was considered. Physical interpretation is that the presence of other fibers around a given test fiber creates a rapid decay of any disturbance velocity that it introduces. Screening length χ was shown to be proportional to "average interparticle spacing for aligned fibers" regardless of orientation:

$$\chi = O[(nL)^{-1/2}]\cdot|\ln\phi|^{1/2} \tag{31}$$

Constant value C'' varies case by case so that to be used as a model is viewed with skepticism despite its sophisticated theoretical derivation.

Also, Phan-Thien and Graham (1991) developed a phenomenological constitutive equation, which implements experimental evidence (Milliken *et al*., 1989; Kitano *et al*., 1981) that at high volume fraction, effective specific viscosity increase with the cube of the volume fraction and modifies Transversely Isotropic Fluid (TIF) model.

$$N = \frac{\phi(L/D)^2(2-\phi/G_v)}{2[\ln(2L/D) - 1.5](1-\phi/G_v)^2} \tag{32}$$

where G_v represents maximum volume fraction;

$$G_v = 0.53 - 0.013L/D, \quad 5 < L/D < 30 \tag{33}$$

5. Fiber-fiber interaction models

There are two possible mechanism of fiber-fiber interaction. At dilute region, as concentration of fiber increases, interactions between neighborhood fibers inhibits regular rotational motion of a given test fiber and thereby increases interaction strength. However, at more concentrated region, as the distance among fibers decreases, rotational motion of the fiber is screened and neighborhood fibers play a role of cage and thereby decreases interaction strength. It corresponds to screening mechanism

5.1. Isotropic diffusivity

Bays model (Bay, 1991)

$$C_I = 0.0184\exp\left(-0.7148\frac{\phi L}{D}\right) \tag{34}$$

According to experimental data, flow-directional orientation is very sensitive to particle volume fraction but out-of-plane component is not. Therefore C_I was determined using experimental data of flow-directional orientation component at steady simple shear flow. To be free from material dependency, three material data were selected and a master curve was found by plotting in terms of $\phi L/D$. Unknown parameter was determined by a least-square fitting technique. However, this model is valid only for concentrated suspension and cannot be used at dilute or semi-dilute suspension. This model definitely shows screening effect.

Ranganathan and Advani's model (Ranganathan and Advani, 1991)

$$C_I = \frac{K}{a_c/L} \tag{35}$$

where K is proportional constant and a_c is average inter-fiber distance. This model represents the tendency of C_I to be variable according to fiber orientation. However, it is not consistent with recent concentrated theories and direct implementation to tensor evolution equation (Eq.9) is impossible due to the necessity of the calculation of average angles among interacting fibers by DFC. So, this model cannot be used as a interaction model for tensorial representation of orientation (Eq.9), yet.

5.2. Anisotropic diffusivity

Sandstrom model (Sandstrom, 1993)

$D(p)$ = correlation time × variance of fiber angular velocity (36)

The correlation time is the expected period over which interaction geometries are uncorrelated. This model also requires the calculation of DFC and contains parameters, which must be determined by experiment. Therefore, to be used as a model is not possible. However, despite the assumptions contained in a model, basic understanding of fiber-fiber interaction effect could be achieved.

Kochs model (Koch, 1995)

$$D_{ij} = \frac{nL^3}{\dot{\gamma}\ln^2(L/D)}(\lambda_1\delta_{ij}\dot{\gamma}_{mn}a_{mnpq}\dot{\gamma}_{pq} + \lambda_2\dot{\gamma}_{rs}a_{rsijuv}\dot{\gamma}_{uv}) \tag{37}$$

This model is based upon a theoretical work on two-body interaction in extensional flow and validated by the dispersion in simple shear flow. In spite of the sophisticated derivation of the model by theoretical and experimental background, it is necessary to closure fourth-order and sixth-order tensor in terms of lower order tensor. There is no available closure approximation for sixth-order and fourth-order orientation tensor for this model. Another closure model must be developed and it is definitely a challenging research topic.

Anisotropic tensor model (Phan-Thien et al., 2000)

$$D_{ij} = C_{ij}\dot{\gamma} \tag{38}$$

where C_{ij} is functions of flow kinematics and expressed as follows :

$$C_{ij} = C_3\delta_{ij} + 2(C_1 - C_3)(A_1)_{ik}(A_1)_{ki}/(A_1)_{ik}(A_1)_{ki} + (C_2 - C_1)(A_2)_{ik}(A_2)_{ki}/(A_2)_{ik}(A_2)_{ki}$$

where $(A_1)_{ij}$ and $(A_2)_{ij}$ are the first two Rivlin-Ericksen tensor:

$$(A_1)_{ij} = \dot{\gamma}_{ij}, \quad (A_2)_{ij} = (\dot{A}_1)_{ij} + (A_1)_{ik}\frac{\partial u_j}{\partial x_k} + \frac{\partial u_i}{\partial x_k}(A_1)_{kj}$$

Constant values C_1, C_2, C_3 were determined by fitting the normal stress data at simple shear flow. More validation of this model is required but it can be criticized that C_{ij} is only functions of flow kinematics and not functions of fiber volume fraction, aspect ratio and orientation.

6. Numerical simulation of fiber orientation in injection molding processes

Many numerical simulations for the prediction of fiber orientation in injection-molded composites are based on the Hele-Shaw approximation (Hieber and Shen, 1980), which neglects the details of the flow field at the melt front, at the boundaries of the plane cavity and at abrupt changes of cavity thickness (e.g., the gate, corners, and sudden contraction or expansion geometries). Fig. 5 shows the test geometry of typical radial diverging flow, center-gated disk. Outer radius is R_o = 76.2 mm and thickness is $2b$ =

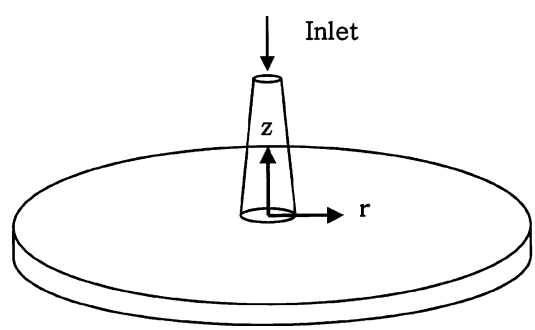

Fig. 5. Mold geometry of center-gated disk.

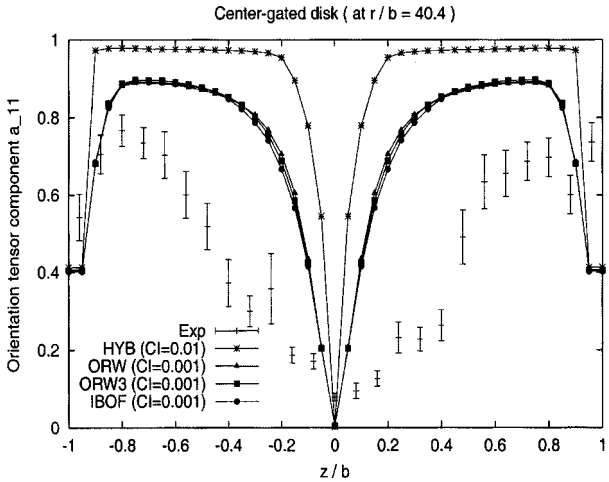

Fig. 6. a_{11} (flow-directional orientation) component as a function of thickness positions (z/b) for various closure approximations of HYB, ORW, ORW3 and IBOF with experimental data for center-gated disk at r/b=40.4.

3.18 mm. The sprue is 20 mm long (not including the total thickness of the disk) and has a radius of 3.81 mm. Shown in Fig. 6 are typical numerical results with the assumption of Hele-Shaw approximation (Chung and Kwon, 2000) for the flow directional orientation component (a_{11}) across the thickness at far downstream of center-gated disk. Experimental data (Bay and Tucker, 1992b) are included. One can observe an over-prediction of flow directional orientation component a_{11} at core layer compared with experimental data (i.e., resulting in too thin core layer). As indicated in Fig. 6, differences among the behaviors of closure approximations (ORW, ORW3 and IBOF) are negligible except HYB, which over-predicts a_{11} compared with other models. It may be mentioned that the predictions near the gate and upto half the outer radius of the disk are in good agreements with experimental data. Thus, while fiber orientation predictions based on the Hele-Shaw approximation show reasonable results far from the melt front regions (Bay and Tucker, 1992a,b; Gupta and Wang, 1993; Verleye and Dupret, 1994; Chung and Kwon, 1995, 1996; Verweyst *et al*., 1997), it is necessary that a complete solution of three-dimensional governing equations including accurate treatment of melt front region is adopted to include significant in-plane deformation rates and out-of-plane velocity components, *etc*.

Filling of two-dimensional (plane or axisymmetric) cases were analyzed by Han (2000). Melt front was tracked using PCM (Pseudo Concentration Method) (Thompson, 1986; Haagh and Vosse, 1998). However, calculated melt front for center gated disk showed unsatisfactory shape and it was due to the corner region where the appropriate wall boundary conditions cannot be applied. First simulations of fiber orientation in three-dimensional molded features, and the first comparisons to experiments, were reported by Verweyst (1998). VOF (Volume of Fluid) method was used to track the melt front. However, for center gated disk simulation, skewing melt front shape was acquired and solutions have diverged.

Recent works by Chung and Kwon (2002b) was to develop a numerical scheme to predict the details of the flow field for an axisymmetric three-dimensional geometry, discarding previous numerical assumptions, such as the Hele-Shaw model. The melt front is captured by the PCM. A finite element method with penalty function formulation is implemented for the solution of incompressible non-Newtonian Stokes flow. Also, non-isothermal effect is included. SUPG (Streamline Upwind Petrov-Galerkin) F.E.M. by Brooks and Hughes (1982) is adopted for the stability of convection-dominated problem. For the fiber orientation prediction, second-order orientation tensor evolution equation (Eq.9) with isotropic diffusivity of $D_r = C_I\dot{\gamma}$ and IBOF closure approximation (Chung and Kwon, 2002a) has been used together with Dinh-Armstrong constitutive model (Dinh and Armstrong, 1984).

6.1. Governing equations

The melt is assumed to be incompressible Stokes flow, hence the governing equations are as follows:

Mass and momentum conservation equations

$$u_{i,i} = 0 \tag{39}$$

$$\sigma_{ij,j} = 0 \tag{40}$$

$$\sigma_{ij} = -P\delta_{ij} + \tau_{ij} \tag{41}$$

where u_i is i-th component of the velocity, σ_{ij} is the Cauchy stress tensor, P is the hydrostatic pressure, δ_{ij} is the identity tensor and τ_{ij} is the deviatoric stress tensor.

Energy equation

$$\rho C_p\left(\frac{\partial T}{\partial t} + u_r\frac{\partial T}{\partial r} + u_z\frac{\partial T}{\partial z}\right) = \frac{1}{r}\frac{\partial}{\partial r}\left(rk_r\frac{\partial T}{\partial r}\right) + \frac{\partial}{\partial z}\left(k_z\frac{\partial T}{\partial z}\right) + \eta\dot{\gamma}^2 \tag{42}$$

where ρ is the density, C_p is the thermal capacity, T is the temperature, k_r, k_z is the thermal conductivity in r-direction and z-direction, respectively and $\eta\dot{\gamma}^2$ is the viscous dissipation. u_r, u_z stands for the velocity component in r-direction and z-direction, respectively.

Pseudo-concentration convection equation

$$F_{,t} + u_i F_{,i} = 0 \tag{43}$$

The distinction between polymer and air (fictitious fluid) is made according to the value of pseudo-concentration func- tion, F. F = 1 corresponds to polymer,

whereas $F = 0$ stands for air. F is tracked by convection with fluid velocity, $\boldsymbol{u}$.

6.2. Numerical methods

Stokes equation

A penalty function method is implemented for the incompressibility constraint and dynamic Robin boundary condition for PCM (Haagh and Vosse, 1998). Elemental matrix equation with stiffness matrix K_{lm} and velocity degree of freedom vector U_m can be obtained as follows:

$$K_{lm}U_m = 0 \tag{44}$$

Bi-linear quadrilateral mesh has been used. For normal domain integration 2×2 Gauss-Legendre rule has been implemented and for other penalty terms, 1-point integration is applied. For the iteration for non-Newtonian flow, Picard (successive substitution) method has been adopted for the stability.

Formulation for time dependent equation including SUPG method

General time-dependent FEM equation by spatial discretization can be expressed as follows:

$$[M]\{\dot{X}\} + [S]\{X\} = \{f\} \tag{45}$$

Temporal discretization is with Crank-Nicholson implicit finite difference method. Solution vector $\{X\}$ can be pseudo-concentration, temperature or fiber orientation components. With regard to SUPG method, artificial diffusion constant $\tilde{k}$ is chosen as follows:

$$\tilde{k} = \frac{c|u|\Delta}{\sqrt{15}} \tag{46}$$

where c is a constant value around unity and Δ is the characteristic mesh size. Also, normalized velocity $\hat{u}_i$ is defined as

$$\hat{u}_i = u_i/|u| \tag{47}$$

Detailed explanations about numerical methods are contained in Chung and Kwon (2002b).

7. Numerical simulation results and discussion

The test geometry of typical radial diverging flow, center-gated disk is shown in Fig. 5. There are 24 finite elements across the thickness and 150 in the radial direction graded towards the sprue. The sprue contains 20 elements uniformly distributed across the radius and 50 elements along its length graded towards the disk. The average fiber length is $L = 210$ μm and the diameter is $D = 11$ μm. Random fiber orientation and parabolic velocity profile is assumed as the inlet boundary condition.

The processing condition is the filling time of 2.5 s, and

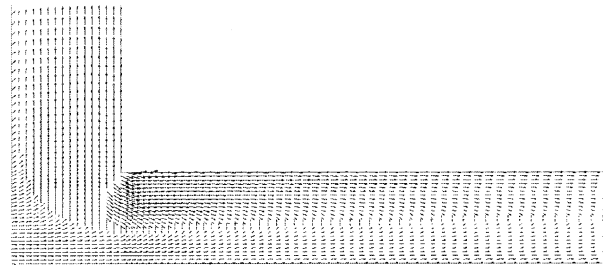

Fig. 7. Typical fiber orientation around sprue junction region.

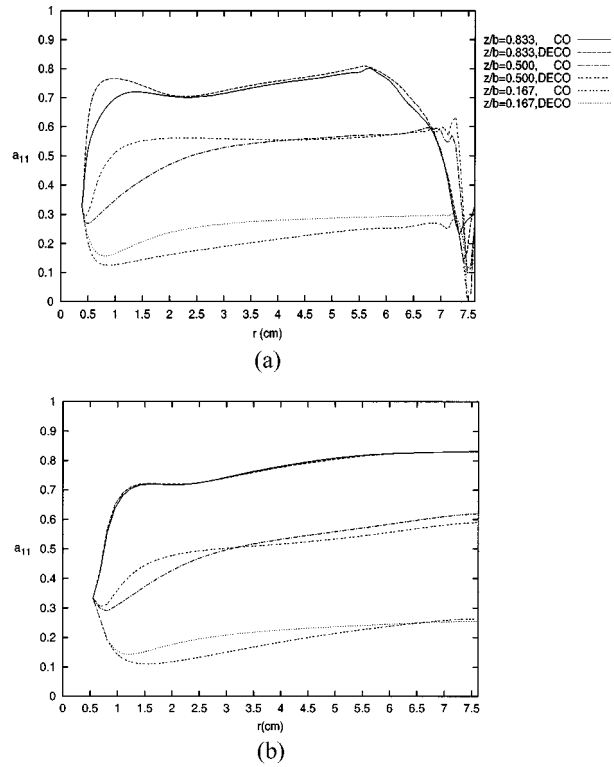

Fig. 8. Coupling effect on a_{11} component for isothermal Newtonian flow (C_I=0.001) as a function of radial positions (r) for center-gated disk (a) including fountain flow (b) neglecting fountain flow.

the viscosity of the Newtonian matrix is 1000 Pa·s. For the analysis of non-isothermal, non-Newtonian matrix, suspension of nylon 6/6 reinforced with 43 wt% ($\phi = 0.23$) of glass fibers (Bay and Tucker, 1992b) was used. Processing conditions includes inlet temperature $T_{inlet} = 550$ K, mold wall temperature $T_{wall} = 347$ K, and the filling time $t_{fill} = 2.5$s. Typical fiber orientation around sprue junction region is depicted in Fig. 7.

7.1. Coupling effect between fluid and fiber

An isothermal Newtonian matrix ($C_I = 0.001$) is assumed and a coupled solution corresponds to $N = 40$; $N = 0$ is a decoupled solution. Fig. 8 shows the coupling effect on the orientation state, implementing IBOF closure approxima-

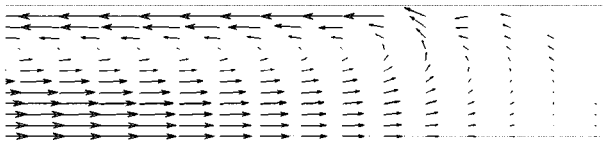

Fig. 9. Predicted velocity plot showing fountain flow around melt front region for non-Newtonian fiber suspension flow (fiber-fluid decoupled case, C_I=0.001). Reference frame is moving with the melt front and the length of arrow indicates relative magnitude of the velocity.

tion, for two different cases: i) taking into account the fountain flow effect (Fig. 8a) and ii) using the Hele-Shaw approximation with the fountain flow effect ignored (Fig. 8b). As indicated in Fig. 8a, the coupling effect on the orientation state is significant in the core and transition layers, even far downstream especially when the fountain flow effect is incorporated. In Fig. 8a, a fountain-flow affected region could be identified by sudden decrease of a_{11} far downstream, and it corresponds to melt front region. On the other hands, Fig. 8b does not show fountain-flow affected region. Therefore, the coupling effect is important near the core and transition layers, even for large *r*. The observation that the coupling effect is more significant around the core and transition layers agrees with the numerical studies by Ranganathan and Advani (1993). And this observation seems to be consistent with the simulations by Chung and Kwon (1996) and Verweyst (1998), which indicated much less effect. Chung and Kwon (1996) performed FEM analysis with the assumption of Hele-Shaw model by implementing HYB closure approximation. They concluded that the coupling effect is only important around the gate region and is negligible throughout the rest of the domain. This restricted effect seems to be mainly due to adopting HYB closure approximation for the prediction of fiber orientation. It might be reminded that, as was seen in Fig. 8b, numerical predictions neglecting fountain flow effect based upon IBOF closure approximation showed qualitatively similar results compared with Fig. 8a. Meanwhile, it may be mentioned that simulation by Verweyst (1998) was failed in advancing the melt front for C_I value below 0.007.

7.2. Fountain flow vs. Hele-Shaw model

Fig. 9 shows the predicted velocity plot for the fountain flow around melt front region and Fig. 10 shows the effect of fountain flow vs. Hele-Shaw model (lubrication approximation) (Chung and Kwon, 1995, 1996) on a_{11} component for non-isothermal non-Newtonian flow (fiber-fluid decoupled case, C_I = 0.001) including experimental data (Bay and Tucker, 1992). Around gate region (at r/b = 5.68) for core (z/b = 0.0~0.3) and transition (z/b = 0.3~0.6) layers, both results show under-predictions of a_{11}. For shell layers (z/b = 0.6~0.9), results including fountain flow almost match the experimental data. As the fluid flows radially

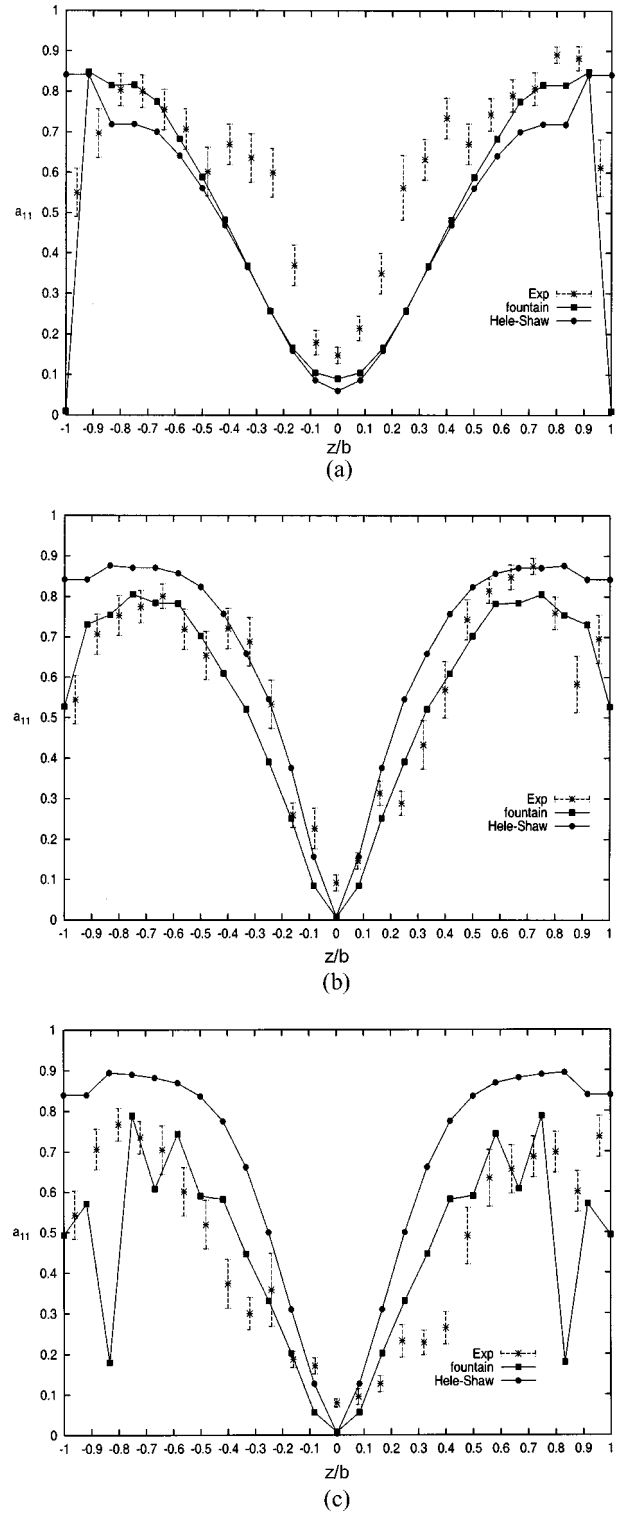

Fig. 10. Effect of fountain flow vs. Hele-Shaw (lubrication approximation) on a_{11} component for non-Newtonian fiber suspension flow (fiber-fluid decoupled case, C_I= 0.001) as a function of thickness positions (z/b) for center-gated disk; (a) at r/b= 5.68 (b) at r/b=22.8 (c) at r/b=40.4.

outward, predictions with fountain flow nearly matches the experimental data. On the other hands, Hele-Shaw model over-predicts a_{11}. Some differences between the numerical results and the experimental data might arise from neglecting packing stage of injection molding cycle. Therefore, fountain flow effect is very crucial for the exact prediction of orientation state and Hele-Shaw model must be discarded.

8. Concluding remarks

We have extensively reviewed recent works on the modeling and simulation of fiber orientation during injection molding processes of short fiber reinforced thermoplastics.

For the closure approximation part, the accuracy of IBOF is as good as EBOF, and computational time for IBOF is only 30~40% of that for EBOF to obtain a solution. Also, IBOF does not suffer from the singularity problems encountered when using the NAT.

Finite element numerical analysis of axisymmetric three-dimensional geometry (including two-dimensional plane case) has been performed for fiber suspensions using Pseudo Concentration method as a melt-front capturing technique. It has been found that including fountain flow effect induces wide core layers of orientation distributions and consequently makes the predictions closer to experimental data. Also, the coupling effect between fluid and fiber is important near the core and transition layers, even for far downstream of the flow direction. For the future, numerical studies of viscoelastic polymer dynamics must accompany with general three-dimensional geometry because of the importance of melt front or gate region on the orientation states. Also, experimental data for various complex geometries must be attained to understand detailed orientation dynamics and rheology.

It is hoped that suspension rheology and particle dynamics be understood for more highly concentrated suspensions in the near future. Then fiber-fiber interaction could be better understood.

9. Acknowledgements

The authors wish to thank the Ministry of Science and Technology for their financial support via the National Research Laboratory Program (2000-N-NL-01-C-148). Also, authors wish to acknowledge the financial support of the Korea Research Foundation made in the program year of (1998) (KRF-1998-005-E00312).

10. List of symbols

a_{ij} = Second-order orientation tensor.
a_{ijkl} = Fourth-order orientation tensor.
a^{p}_{ijkl} = Fourth-order orientation tensor in reference to eigenspace of second-order orientation tensor (Defined to be principal values of fourth-order orientation tensor in this paper).
a_1, a_2, a_3 = Eigenvalues of second-order orientaton tensor in descending order in magnitude.
a_c = Average inter-fiber spacing.
A_{mm} = Principal values of fourth-order orientation tensor in contracted notation.
$(A_1)_{ij}$, $(A_2)_{ij}$ = First two Rivlin-Ericksen tensor.
b = Half gap thickness of molded part.
C_I = Interaction coefficient for fiber-fiber interaction.
C_p = Thermal capacity of the thermoplastic medium.
D = Fiber diameter.
D_r = Diffusivity term which accounts for fiber-fiber interaction.
D_{ij} = Anisotropic diffusivity tensor.
f = Scalar measure of orientation.
F = Pseudo Concentration Function.
G_v = Maximum volume fraction of fiber.
h = Average distance from a given fiber to its nearest neighbor.
k = Thermal conductivity of the thermoplastic medium.
$\tilde{k}$ = Artificial diffusion constant for SUPG.
K = A universal constant of proportionality.
L = Fiber length.
n = Number of fibers per unit volume.
N = Dimensionless number accounting for anisotropic contribution from fiber.
p = Fiber unit direction.
$\dot{p}_i$ = Fiber angular velocity.
P = Pressure.
Q = Inlet volume flow rate.
R_i = Inlet radius of center-gated disk.
R_0 = Outer radius of center-gated-disk.
t_{fill} = Filling time.
T = Temperature.
T_{inlet} = Inlet melt temperature.
T_{wall} = Mold wall temperature.
u_i = Velocity component in ith direction.
$u_{i,j}$ = $\partial u_i / \partial x_j$, velocity gradient tensor.
D/Dt = Material derivative.
I,II,III = First, second and third principal invariants of a_{ij}.
$\Psi(\boldsymbol{p})$ = Probability distribution function.
$\dot{\gamma}$ = Generalized shear rate.
$\dot{\gamma}_{ij}$ = Rate of deformation tensor.
δ_{ij} = Unit tensor.
η = Viscosity of the thermoplastic medium.
ϕ = Volume fraction of fibers.
λ = Geometric parameter related to the particle aspect ratio.
χ = Screening length.

ρ = Density of the thermoplastic medium.
σ_{ij} = Cauchy stress tensor.
τ_{ij} = Deviatoric stress tensor.
ω_{ij} = Vorticity tensor.

References

Advani S.G. and C.L. Tucker III, 1987, The use of tensors to describe and predict fiber orientation in short fiber composites, *J. Rheol.* **31**, 751-784.

Advani S.G. and C.L. Tucker III, 1990, closure approximations for three-dimensional structure tensors, *J. Rheol*. **34**(3), 367-386.

Batchelor G.K., 1971, The stress generated in a non-dilute suspension of elongated particles by pure straining motion, *J. Fluid Mech*. **46**, 813-829.

Bay R.S., 1991, Ph.D thesis, Fiber orientation in injection molded composites : A comparison of theory and experiment, University of Illinois at Urbana-Champaign, U.S.A.

Bay R.S. and C.L. Tucker III, 1992a, Fiber orientation in simple injection moldings. Part I: Theory and numerical methods, *Polym.Compos.* **13**(4), 317-331.

Bay R.S. and C.L. Tucker III, 1992b, Fiber orientation in simple injection moldings. Part II: Experimental results, *Polym.Compos.* **13**(4), 332-341.

Brooks, A.N. and T.J.R. Hughes, 1982, Streamline Upwind/ Petrov-Galerkin Formulations for Convection Dominated Flows with Particular Emphasis on the Incompressible Navier-Stokes Equations, *Comp. Meth. Appl. Mech. Eng*. **32**, 199-259.

Chung D.H. and T.H. Kwon, 1999, Improved Orthotropic Closure Approximation for Fiber Orientation Tensorial Description, in P.G.M. Kruijt, H.E.H. Meijer, F.N. van de Vosse (Eds.), PPS15 Proceedings, Paper 180, Eindhoven University of Technology, Eindhoven

Chung D.H. and T.H. Kwon, 2000, Applications of Recently Proposed Closure Approximations to Injection Molding Filling Simulation of Short-fiber Reinforced Plastics, *Korea-Australia Rheology Journal* **12**(2), 125-133.

Chung D.H. and T.H. Kwon, 2001, Improved Model of Orthotropic Closure Approximation for Flow Induced Fiber Orientation, *Polym. Compos*. **22**(5), 636-649.

Chung D.H. and T.H. Kwon, 2002a, Invariant-based optimal fitting closure approximation for the numerical prediction of flow-induced fiber orientation, *J.Rheol.* **46**(1), 169-194.

Chung D.H. and T.H. Kwon, 2002b, Numerical Studies of Fiber Suspensions in an Axisymmetric Radial Diverging Flow: The Effects of Modeling and Numerical Assumptions, J. Non-Newtonian Fluid Mech. **107**, 67-96.

Chung S.T. and T.H. Kwon, 1995, Numerical Simulation of Fiber Orientation in Injection Molding of Short-Fiber-Reinforced Thermoplastics, *Polym. Eng.Sci*. **35**, 604-618.

Chung S.T. and T.H. Kwon, 1996, Coupled Analysis of Injection Molding Filling and Fiber Orientation Including In-Plane Velocity Gradient Effect, *Polym. Compos.* **17**, 859-872.

Cintra J.S. and C.L. Tucker III, 1995, Orthotropic Closure Approximations for Flow-Induced Fiber Orientation, *J. Rheol*. **39**, 1095-1122.

Dinh S.M. and R.C. Armstrong, 1984, A Rheological Equation of State for Semiconcentrated Fiber Suspensions, *J. Rheol*. **28**(3), 207-227.

Dupret F. and V. Verleye, 1999, Modelling the flow of fiber suspensions in narrow gaps, in Advances in the Flow and Rheology of Non-Newtonian Fluids, D.A.Siginer, D.De Kee and R.P.Chhabra (Eds.), Rheology Series, 8, Elsevier, Amsterdam, p19-29.

Fan X.J., N. Phan-Thien and R. Zheng, 1998, A Direct Numerical Simulation of Fibre Suspensions, *J.Non-NewtonianFluid Mech.* **74**, 113-135.

Folgar F. and C.L. Tucker III, 1984, Orientation Behavior of Fibers in Concentrated Suspensions, *J.Reinf. Plast.Compos.* **3**, 98-119.

Gupta, M. and K.K.Wang, 1993, Fiber orientation and mechanical properties of short-fiber-reinforced injection-molded composites: Simulated and experimental results, *Polym. Compo*. **14**, 367-382.

Haagh, G. A.A.V. and F.N.V.D. Vosse, 1998, Simulation of Three-Dimensional Polymer Mould Filling Processes Using a Pseudo-Concentration Method, *Int. J. Numer. Meth.Fluids* **28**, 1355-1369.

Halpin J.C. and J.L. Kardos, 1976, "The Halpin-Tsai Equations: A Review", *Polym. Eng. Sci.* **16**, 344-352.

Han, K.H. and Y.T. Im, 1999, Modified hybrid closure approximation for prediction of flow-induced fiber orientation, *J. Rheol*. **43**(3), 569-589.

Han, K.H., 2000, Ph.D thesis, Enhancement of Accuracy in Calculating Fiber Orientation Distribution in Short Fiber Reinforced Injection Molding, Department of Mechanical Engineering, Korea Advanced Institute of Science and Technology, South Korea.

Hieber C.A. and S.F. Shen, 1980, A finite-element/finite-difference simulation of the injection-molding filling process, *J. Non-Newtonian Fluid Mech.* **7**, 1-32.

Hinch E.J. and L.G. Leal, 1972, The effect of Brownian motion on the rheological properties of a suspension of non-spherical particles, *J. Fluid Mech.* **52**, 683-712.

Jeffery G.B., 1922, The Motion of Ellipsoidal Particles Immersed in a Viscous Fluid, *Proc. R.Soc.* **A102**, 161-179.

Kitano T., T. Kataoka and T. Shirota, 1981, An empirical equation of the relative viscosity of polymer melts filled with various inorganic fillers, *Rheol. Acta* **20**, 207-209.

Koch D.L., 1995, A model for orientational diffusion in fiber suspensions, Phys. Fluids, **7**, 2086-2088.

Mackaplow M.B. and E.S.G. Shaqfeh, 1996, A Numerical Study of the Rheological Properties of Suspensions of Rigid, non-Brownian Fibres, *J.Fluid Mech.* **329**, 155-186.

Milliken W.J., M. Gottlieb, A.L. Graham, L.A. Mondy and R.L. Powell, 1989, The viscosity-volume fraction relation for suspensions of rod-like particles by falling-ball rheometry, *J. Fluid Mech.* **202**, 217-232.

Phan-Thien N. and A.L. Graham, 1991, A new constitutive model for fibre suspensions : flow past a sphere, *Rheol. Acta* **30**, 44-57.

Phan-Thien N., X.J. Fan and R. Zheng, 2000, A numerical sim-

ulation of suspension flow using a constitutive model based on anisotropic interparticle interactions, *Rheol. Acta* **39**, 122-130.

Ranganathan S. and S.G. Advani, 1991, Fiber-fiber interactions in homogeneous flows of nondilute suspensions, *J.Rheol*. **35**(8), 1499-1522.

Ranganathan S. and S.G. Advani, 1993, A simultaneous solution for flow and fiber orientation in axisymmetric diverging radial flow, *J. non-Newtonian Fluid Mech*. **47**, 107-136.

Sandstrom C.R., 1993, Ph.D thesis, Interactions and orientation in concentrated suspensions of rigid rods: Theory and experiment, University of Illinois at Urbana-Champaign, U.S.A.

Shaqfeh E.S.G. and G.H. Fredrickson, 1990, The Hydrodynamic Stress in a Suspension of Rods, *Phys.Fluids* **A 2**(1), 7-24.

Sundararajakumar R.R. and D.L. Koch, 1997, Structure and Properties of Sheared Fiber Suspensions with Mechanical Contacts, *J.Non-Newtonian Fluid Mech*. **73**, 205-239.

Thompson, E., 1986, Use of Pseudo-Concentrations to Follow Creeping Viscous Flows during Transient Analysis, *Int. J. Numer. Meth. Fluids* **6**, 749-761.

Wetzel E.D., 1999, Ph.D thesis, Modeling Flow-Induced Microstructure of Inhomogeneous Liquid-Liquid Mixtures, University of Illinois at Urbana-Champaign, U.S.A.

Verleye, V. and F. Dupret, 1994, Numerical Prediction of Fiber Orientation in Complex Injection Molded Parts, Proc. of the ASME Winter Annual Mtg. MD-Vol49. HTD-Vol283, p.264-279.

Verweyst, B.E., C.L. Tucker III, and P.H. Foss, 1997, The optimized quasi-planar approximation for predicting fiber orientation in injection-molded composites, *Int. Polym. Process*. **12**(3), 238-248.

Verweyst B.E., 1998, Ph.D thesis, Numerical Predictions of Flow-Induced Fiber Orientation in Three-Dimensional Geometries, University of Illinois at Urbana-Champaign, U.S.A.

Yamamoto S. and T. Matsuoka, 1993, A Method for Dynamic Simulation of Rigid and Flexible Fibers in a Flow Field, *J. Chem. Phys*. **98**(1), 644-650.

Yamane Y., Y. Kaneda Y. and M. Doi, 1994, Numerical Simulation of Semi-dilute Suspensions of Rodlike Particles in Shear Flow, *J. Non-Newtonian Fluid Mech.* **54**, 405-421.